Finite-frequency magnetoelectric response of three-dimensional topological insulators

Adolfo G. Grushin[1] and Fernando de Juan[2]
[1]*Instituto de Ciencia de Materiales de Madrid, CSIC, Cantoblanco, E-28049 Madrid, Spain*
[2]*Department of Physics, Indiana University, Bloomington, Indiana 47405, USA*
(Received 8 March 2012; published 16 August 2012)

Topological insulators with a time-reversal symmetry-breaking perturbation near the surface present a magnetoelectric response that is quantized when the frequency of the probing fields is much smaller than the surface gap induced by the perturbation. In this work we describe the intrinsic finite-frequency magnetoelectric response of topological insulators for frequencies of the order of and larger than the surface gap, including the experimentally relevant case where the system is metallic. This response affects physical observable quantities and will give rise to new finite-frequency phenomena of intrinsic topological origin.

DOI: 10.1103/PhysRevB.86.075126 PACS number(s): 75.85.+t, 72.10.−d

I. INTRODUCTION

It is well understood[1] that under a time-dependent external electromagnetic perturbation any given material will develop a time-dependent response whenever the characteristic frequencies of the perturbation are larger than the characteristic frequencies that induce a polarization or a magnetization in the material. The linear response of conventional dielectrics is characterized by a dielectric function $\varepsilon(\omega)$ and a magnetic permeability $\mu(\omega)$. There is, in fact, a wider class of materials, known as magnetoelectric materials,[2] which effectively introduce other response functions that couple electric and magnetic fields and which, in general, can also depend on the frequency. Perhaps the most striking case of the latter is the recently discovered three-dimensional topological insulators (TI).[3,4] They have been predicted to host a quantized magnetoelectric term in the action, topological in origin,[5,6] of the form $S = \int dt d^3x (\alpha/4\pi^2)\theta \mathbf{E}\cdot\mathbf{B}$, where $\alpha = e^2/\hbar c$ and $\theta = \pi$, which is only physically relevant when time-reversal symmetry is broken, which implies that the surface states that characterize these materials are gapped. Despite the fact that this term remains experimentally elusive, there has been much ongoing work on its consequences. It has been predicted to give rise to a plethora of phenomena, including the Kerr and Faraday rotation of light determined by the fine-structure constant[7,8] and a repulsive Casimir effect,[9,10] where the region of repulsion is determined by θ. Physically, these approaches are valid only when the frequencies of the relevant fields are much smaller than the surface gap m and the topological magnetoelectric term θ is independent of the frequency and quantized. In general, the magnetoelectric response will depend on the frequency and permeate into physical observables, just as the dielectric function or the magnetic permeability does, modifying all the described phenomena related to this topological term.

In this work, we derive the finite-frequency magnetoelectric response of a model Hamiltonian which captures the basic features of a three-dimensional TI. To do so, we will generalize the method introduced in Ref. 5 to finite frequency, relating the response of TIs to that of an effective model with an extra dimension that behaves as a higher-dimensional analog of the quantum Hall effect (QHE).[11] This approach has been shown to be helpful to understand the topological origin of this response, and it is also an efficient computational tool in practice. It has proven useful to predict the magnetoelectric response in a related physical situation[12–14] where the bulk of the TI is assumed to be doped. In this particular case, the magnetoelectric response is not quantized if the chemical potential is outside the band gap, a behavior that may be interpreted as arising from the corresponding anomalous QHE analog in five dimensions.

Here we extend these analyses to a more general and potentially relevant experimental situation where both the frequency and the chemical potential are kept finite, a case that can also be understood as descending from a five-dimensional finite-frequency QHE at finite chemical potential. As a consistency check we will show how known results are recovered in the appropriate limits, giving further physical insight into them.

II. THE MODEL

Consider the lattice Hamiltonian introduced in Ref. 5, which captures the low-energy description of a generic TI, for instance, Bi_2Se_3.[13,15] This Hamiltonian can be written as $H = H_0 + H_M$, with

$$H_0 = t\sum_{\mathbf{x},s} c^\dagger_{\mathbf{x}}\frac{\Gamma_0 - i\Gamma_s}{2}c_{\mathbf{x}+\hat{\mathbf{s}}} + \text{H.c.} - 3tc^\dagger_{\mathbf{x}}\Gamma^0 c_{\mathbf{x}}, \quad (1)$$

$$H_M = M\sum_{\mathbf{x}} c^\dagger_{\mathbf{x}}\Gamma^0 c_{\mathbf{x}}, \quad (2)$$

with $\mathbf{x}$ running through all unit cells, $s = 1,2,3$, and where $\hat{\mathbf{s}}$ is the lattice vector in the s direction. Γ_μ are defined as the set of 4×4 matrices that satisfy $\{\Gamma_\mu,\Gamma_\nu\} = 2\delta_{\mu\nu}$, with $\mu,\nu = 0,1,2,3,4$, including an extra Γ_4 that will be used shortly. In momentum space this can be written as

$$H(\mathbf{k}) = \left(t\sum_{s=1}^{3}\cos(k_s) + M - 3t\right)\Gamma_0 + t\sum_{s=1}^{3}\sin(k_s)\Gamma_s. \quad (3)$$

These models can be thought of as lattice models that host an odd number of low-energy massive Dirac fermions.[16] For example, for $|M| < t$ there is a single Dirac fermion at $\mathbf{k} = 0$ of gap M.

The presence of a boundary in the Hamiltonian can be modeled by making the gap position dependent,

 ©2012 American Physical Society

promoting (2) to

$$H_M = \sum_{\mathbf{x}} M \cos\theta(\mathbf{x}) c^\dagger_{\mathbf{x}} \Gamma_0 c_{\mathbf{x}}. \quad (4)$$

This accounts for the band inversion by setting $\theta(-\infty) = \pi$ in the bulk of the TI and $\theta(\infty) = 0$. The specific dependence of θ on x will not be needed for our purposes, only its asymptotic values. Both experimentally[17] and from *ab initio* calculations[15] the bulk band gap is well approximated by $M = 0.3$ eV for Bi_2Se_3. A time-reversal symmetry-breaking perturbation may generically be included as[12]

$$H_m = \sum_{\mathbf{x}} m \sin\theta(\mathbf{x}) c^\dagger_{\mathbf{x}} \Gamma_4 c_{\mathbf{x}}, \quad (5)$$

which is localized at the boundary and opens a surface gap m. This surface gap can arise from doping the TI with magnetic impurities and has been measured to be $m \sim 50$ meV.[18,19]

III. FINITE-FREQUENCY ELECTROMAGNETIC RESPONSE OF A TOPOLOGICAL INSULATOR

To obtain the finite-frequency response of a TI system to electromagnetic fields in the presence of $\theta(x)$, we will first generalize the original procedure devised in Ref. 5 to finite frequency. In what follows, we compute the current response of the system with a generalized Kubo formula in a way that the effect of $\theta(x)$ is included in a manifestly perturbative fashion along the derivation. Our starting point is to consider the current density at some particular point in space-time x_0:

$$j^\mu(x_0) = \frac{\delta S}{\delta A_\mu(x_0)}, \quad (6)$$

where S is the action functional of the system. For a profile $\theta(x)$ that is smooth over length scales $l_m \equiv 1/(v_F m)$ (that is, $|\vec{\nabla}\theta| \ll 1/l_m$), the current at x_0 is mainly determined by θ around $\theta(x_0) \equiv \theta_0$ because correlation functions decay exponentially with l_m. We may therefore include its effects in perturbation theory in $\partial_i\theta$, which is, by assumption, small. For the calculation of $j^\mu(x_0)$, we thus approximate[12]

$$\theta(x) \approx \theta(x_0) + \partial_i\theta|_{x=x_0}\left(x^i - x^i_0\right) + \cdots \quad (7)$$

in the Hamiltonian $H = H_0 + H_M + H_m$ defined by Eqs. (1), (4), and (5), respectively. To first order in $\partial_i\theta$ the mass terms read

$$\begin{aligned} H_M + H_m = &\sum_{\mathbf{x}} c^\dagger_{\mathbf{x}}(M\cos\theta_0\Gamma_0 + m\sin\theta_0\Gamma_4)c_{\mathbf{x}} \\ &+ \partial_i\theta|_{\mathbf{x}_0}\sum_{\mathbf{x}}\left(x^i - x^i_0\right)c^\dagger_{\mathbf{x}}(-M\sin\theta_0\Gamma_0 \\ &+ m\cos\theta_0\Gamma_4)c_{\mathbf{x}}. \end{aligned} \quad (8)$$

Note that in this Hamiltonian θ_0 is just a constant parameter.

We can now compute the current response at x_0 when a time-dependent uniform electric field is applied to the system. This is done by computing the expectation value of j^μ to first order in both $\partial_i\theta$ and the electromagnetic field A_μ, with a generalized Kubo formula:

$$j^i(x_0) = \partial_s\theta|_{\mathbf{x}_0}\sum_{x,x'}\left\langle \hat{J}^i(x_0)\hat{J}^j(x)\hat{J}^s_\theta(x')\right\rangle A_j(x), \quad (9)$$

where $i,j,s = 1,2,3$, repeated indices summation is implied, and x_0,x,x' are full space-time variables. In this expression $\hat{J}^i(x)$ are the current operators, and $\hat{J}^s_\theta(x)$ is the operator attached to $\partial_s\theta$ in Eq. (8) which defines the following vertex in momentum space:

$$J^s_\theta(k) = (-M\sin\theta_0\Gamma_0 + m\cos\theta_0\Gamma_4)\partial_{k_s} \equiv J_\theta\partial_{k_s}. \quad (10)$$

With this, the Fourier transform of the current reads

$$\begin{aligned} j^i(x_0) = &\ \partial_s\theta|_{\mathbf{x}_0}\int_{\rm BZ}\frac{d^4p}{(2\pi)^4}e^{-ipx_0}A^j_p\int_{\rm BZ}\frac{d^4k}{(2\pi)^4} \\ &\times\left[{\rm Tr}\,J^i_{k-p/2}G_{k-p}J^j_{k-p/2}G_kJ_\theta\partial_{k_s}G_k \right.\\ &\left.+\left\{\begin{matrix} p \longleftrightarrow -p \\ i \longleftrightarrow j\end{matrix}\right\}\right], \end{aligned} \quad (11)$$

where the integral spans the entire Brillouin zone (BZ). The electronic Green's function, which depends on a four-momentum vector $k = (k_0,\mathbf{k})$, is given by $G(k,\theta_0) = [k_0 - H(\mathbf{k},\theta_0)]^{-1}$, defined through the Fourier-transformed Hamiltonian

$$H(\mathbf{k},\theta_0) = H(\mathbf{k}) + (M\cos\theta_0\Gamma_0 + m\sin\theta_0\Gamma_4), \quad (12)$$

which depends parametrically on θ_0, the bulk mass M, and the surface mass m. The current vertices are defined as $J^i(k) = \frac{\partial H(\mathbf{k},\theta_0)}{\partial k_i}$, $J^0 = \mathrm{I}_{4\times4}$, with $i = 1,2,3$. In the derivation we have omitted terms arising from vertices with higher derivatives of $H(\mathbf{k},\theta_0)$ with respect to k (Ref. 20) that will not contribute to the magnetoelectric response.

Before we proceed further, it is worth noting that this equation may also be written as

$$j^i(x_0) = \partial_s\theta|_{\mathbf{x}_0}\int_{\rm BZ}\frac{d^4p}{(2\pi)^4}e^{-ipx_0}\partial_{q_s}\left[\Pi^{ij}_4(p,q,\theta_0)\right]_{q=0}A^j_p, \quad (13)$$

where

$$\begin{aligned} \Pi^{\mu\nu}_4(p,q,\theta_0) = &-ie^2\int_{\rm BZ}\frac{d^4k}{(2\pi)^4}\left[{\rm Tr}\,J^i_{k-(p+q)/2}G_{k-p}J^j_{k-p/2}\right.\\ &\left.\times G_kJ_\theta G_{k-q} + \left\{\begin{matrix} p \longleftrightarrow -p+q \\ i \longleftrightarrow j\end{matrix}\right\}\right], \end{aligned} \quad (14)$$

and again the identity holds, disregarding higher derivatives of $H(\mathbf{k},\theta_0)$. $\Pi^{ij}_4(p,q)$ can be considered the response function to $\delta\theta = \theta_0 - \theta(x)$,

$$j^i(x_0) = \int_{\rm BZ}\frac{d^4p}{(2\pi)^4}\frac{d^4q}{(2\pi)^4}e^{-i(p+q)x_0}\Pi^{ij}_4(p,q,\theta_0)A^j_p\delta\theta_q, \quad (15)$$

which is the generalization to finite frequency and momenta of Ref. 5. Equation (11) represents an equivalent statement that features an explicit small parameter throughout the derivation.

Consider now the case where the boundary of the TI is in the z direction, so that $\theta(\mathbf{x}) = \theta(z)$. A uniform but time-dependent electric field E_j in momentum space can be written in terms of an external vector potential A_i that is constant in space, so that $A_i(p_0,\mathbf{p}) = \delta(\mathbf{p})A_i(p_0)$.

The total current density in the xy plane, shown to be quantized in the dc limit,[5,12] is defined as $\mathcal{J}^i_{2D} = \int dz j^i(z)$, with $i = x,y$. The finite-frequency generalization of this quantity, i.e., the integrated current density, thus reads

$$\mathcal{J}^i_{2D}(p_0) = \int dz_0\partial_{z_0}\theta(z_0)\partial_{q_z}\left[\Pi^{ij}_4(p,q,\theta_0)\right]_{q=0,\mathbf{p}=0}A^j_{p_0}. \quad (16)$$

With the change of variables $\int_{-\infty}^{\infty} dz_0 \partial_{z_0}\theta = \int_{-\pi}^{0} d\theta$ the current is finally

$$\mathcal{J}^i_{2D}(p_0) = 2\pi \int_{-\pi}^{0} \frac{d\theta}{2\pi} \partial_{q_z}\left[\Pi_4^{ij}(p,q,\theta)\right]_{q=0,\mathbf{p}=0} A^j_{p_0}. \quad (17)$$

As in the static case, the parameter θ can be thought of as the fifth coordinate of a 4+1 model described by $H(\mathbf{k},\theta)$, whose response functions are integrated only over half of the BZ because $0 \leqslant \theta \leqslant \pi$. The topological finite-frequency response of a three-dimensional TI is thus intimately related to the finite-frequency response of a $D = 4 + 1$ insulator.

Consider now the experimentally relevant limit where $m \ll M$. In this limit the response in Eq. (17) can be obtained analytically. This is due to the fact that the low-energy physics of Hamiltonian (12), considered now as a $4 + 1$ Hamiltonian in half of the BZ, is dominated by an effective $4 + 1$ Dirac fermion of gap m located at $(\mathbf{k},\theta) = (0,\pi/2)$, where the $4 + 1$ analog of the Berry curvature is largest. Integrals in the five-dimensional BZ are thus well approximated by a region of momenta around $(0,\pi/2)$ within some cutoff Λ, and the effective Hamiltonian in the vicinity of that point is given by

$$\begin{aligned} H(\mathbf{k},\theta) &\approx H(0,\pi/2) + \partial_{k_i} H|_{(0,\pi/2)} k_i + \partial_\theta H|_{(0,\pi/2)}\tilde{\theta} \\ &= \Gamma^i k_i + M\tilde{\theta}\Gamma^0 + m\Gamma^5, \end{aligned} \quad (18)$$

with $\theta = \pi/2 + \tilde{\theta}$. We can identify this Hamiltonian as that of a $4+1$ Dirac fermion where $k_4 = M\tilde{\theta}$. The cutoff for this model is of order $\Lambda \approx M$, and for $\omega \ll M$ it may be taken to infinity. Within this approximation, the θ integral in Eq. (17) is

$$\begin{aligned} \Pi_5^{ij0}(p,q) \equiv \int_{-\pi}^{0} \frac{d\theta}{2\pi} \Pi_4^{ij}(p,q,\theta) &\approx \frac{-ie^2}{M} \int^{\infty} \frac{d^5k}{(2\pi)^5} \\ &\times \mathrm{Tr}\big[\Gamma^i G_{k-p} \Gamma^j G_k M\Gamma^0 G_{k-q} \\ &+ \Gamma^j G_{k+p-q} \Gamma^i G_k M \Gamma^0 G_{k-q}\big], \end{aligned} \quad (19)$$

where we have used $d\tilde{\theta} = dk_4/M$ and Eq. (14) with the current vertices approximated around $(0,\pi/2)$: $J^i = \Gamma^i$, $J^\theta = M\Gamma^0$. The Green's functions in these expressions are those of a $4+1$ Dirac fermion, obtained as $G(k) = [k_0 - H(\mathbf{k})]^{-1}$ from Eq. (18), where now $\mathbf{k}$ has four components. Consequently, the function Π_5^{ij0} corresponds to the Dirac fermion triangle diagrams shown in Fig. 1, which can be computed analytically with standard methods that are detailed in Appendix A (see also Ref. 21) and can be considered as the optical response of the five-dimensional analog of the QHE. The magnetoelectric response is given by the antisymmetric part of the diagram, and thus the total current finally reads

$$\begin{aligned} \mathcal{J}^i_{2D}(p_0) &= 2\pi\,\Pi_5(p_0,\mu)\epsilon^{ij} E_j(p_0) \\ &\equiv \sigma(p_0,\mu)\epsilon^{ij} E_j(p_0), \end{aligned} \quad (20)$$

where the function

$$\Pi_5(p,q) = \frac{\epsilon_{ij}}{2} \frac{1}{p_0} \partial_{q_z}\left[\Pi_5^{ij0}(p,q)\right]_{q=0,\mathbf{p}=0}, \quad (21)$$

and we have used $E^j_p = ip_0 A^j_p$. Equations (20) and (21) define the finite-frequency response of a TI, which we proceed to evaluate in the next section for different experimentally relevant scenarios.

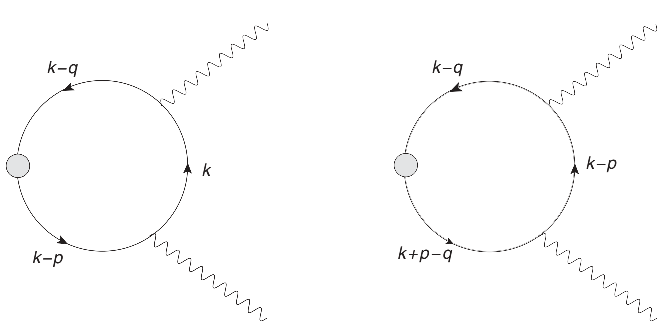

FIG. 1. Feynman diagrams corresponding to Eq. (19). The second diagram is obtained from the first by $i \leftrightarrow j$ and $p \leftrightarrow -p + q$. The gray dot represents the $\partial_s\theta$ vertex.

IV. RESULTS

In this section we compute the function $\sigma(p_0,\mu)$ defined above which determines the response of the TI to an external electromagnetic field of finite frequency. First, it is possible to restore the dependence on the chemical potential since nothing in the above argument depends on whether or not the chemical potential is finite as long as $\mu \ll M$. For a massive Dirac fermion at zero chemical potential, the function $\Pi_5(p_0,\mu = 0)$ can be analytically computed. The final analytical expression at which one arrives depends only on the surface gap m and is given by (we refer the reader to Appendix A for details)

$$\sigma(p_0,\mu = 0) = \frac{1}{2}\frac{e^2}{h}\frac{m}{p_0} \log\left|\frac{2m + p_0}{2m - p_0}\right|. \quad (22)$$

This function, plotted in Fig. 2, governs the finite-frequency response of a TI and is one of the central results of this work. The quantization of the real part at low frequencies is broken down at finite frequency, giving rise to a logarithmic divergence at $p_0 = 2m$. Therefore, close to this range of frequencies, the θ term will dominate the electromagnetic response of the TI. This is particularly important for Casimir-type experiments,[9,10] where the interplay between the optical properties of ordinary and topological response determines not only the sign of the force but also at what distance the crossover between attractive and repulsive behavior happens. The precise way this response alters the Casimir force is an interesting issue on its own, and it is left for a future study.

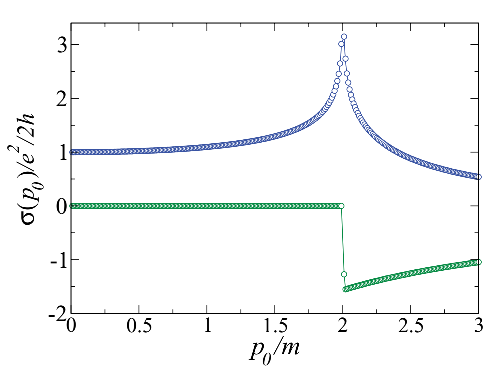

FIG. 2. (Color online) Real (top) and imaginary (bottom) parts of $\sigma(p_0,\mu = 0)$ given by Eq. (22) as a function of p_0 in units of the surface gap m. The quantization is lost at higher frequency, and a logarithmic singularity appears at $p_0 = 2m$.

It is important to note that the analytic result (22) coincides exactly with the optical Hall conductivity of a massive ($D = 2 + 1$)-dimensional Dirac fermion. The dc response of a single Dirac fermion is quantized to $e^2/2h$, which is consistent with the fact that in the lattice model the integrals span only half of the BZ. We thus recover the well-known result that the boundary of a TI with broken time-reversal symmetry hosts a half-integer quantum Hall effect.

Being precise, this result should not be interpreted as if there is a massive $D = 2 + 1$ Dirac fermion somewhere in the system. Instead, these results imply that the three-dimensional optical response of a TI is characterized by spatial average in the z direction of all the $\sigma_{xy}(z)$ Hall conductivities that occur wherever there is a nonzero gradient of $\partial_z\theta(z)$. This situation is relevant for the recent experiments described in Refs. 18 and 19, where TI are doped with magnetic impurities that break time-reversal symmetry. It is remarkable nevertheless that a full $D = 3 + 1$ calculation reduces to a $D = 2 + 1$ result. As will be shown immediately below, this statement does not hold for the case of finite chemical potential.

To clarify the role of a finite chemical potential, one should compute $\Pi_5(p_0,\mu)$. This can be exactly evaluated for some cases which we proceed to describe (technical details are left for Appendix B). One of them is the dc response at finite μ. This limit was discussed earlier in Refs. 12–14 and has obvious interest on its own since TI appear naturally doped in experiments. The numerical evaluation for $\Pi_5(p_0 \to 0,\mu)$ in the dc limit is exactly given for our model by the expression

$$\sigma(p_0 \to 0,\mu) = \frac{e^2}{h}\begin{cases} \frac{1}{2}\mathrm{sgn}(m) & \text{if} \quad |\mu| \leqslant m, \\ \frac{1}{4}\left[\frac{3m}{|\mu|} - \frac{m^3}{|\mu|^3}\right] & \text{if} \quad |\mu| \geqslant m. \end{cases} \tag{23}$$

The result is shown in Fig. 3(a). The analytical expression reveals that although there is a quantized value at values of $|\mu| \leqslant m$ which also occurs for $D = 2 + 1$ fermions,[22,23] already one can notice very important differences with respect to the $D = 2 + 1$ case. In $D = 2 + 1$ it can be shown[22,23] that only a term $m/|\mu|$ arises at fillings larger than the gap. In the present case, however, there is a second term which has a different behavior and scales like $m^3/|\mu|^3$. This term is therefore intrinsically related to the $D = 3 + 1$ nature of the carriers, which is only fully transparent in the analytic result. The extra term turns the kink between the two regimes $|\mu| \leqslant m$ and $|\mu| \geqslant m$ smoother, making the curve in Fig. 3(a) differentiable at all μ, in contrast with the $2 + 1$ result.

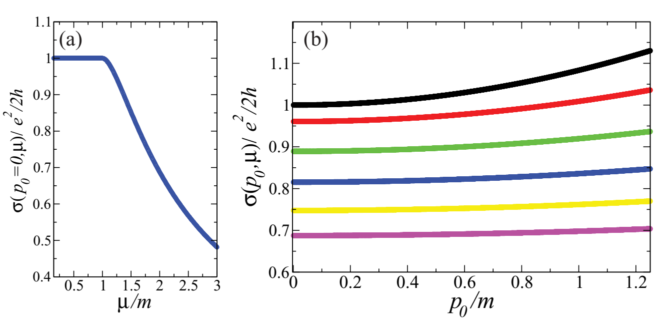

FIG. 3. (Color online) $\sigma(p_0,\mu)$ as a function of (a) the chemical potential μ for zero frequency in units of the surface gap m and (b) the external frequency p_0 for $\mu/m = 1.0$–2.0 in steps of 0.2 (top to bottom). There is a quantization plateau whenever $|\mu| \leqslant m$ and a decay for $\mu \geqslant m$ given by (23). For finite frequencies and whenever $|\mu| \geqslant m$ is satisfied, the dc value is not quantized and is given by Eq. (24).

Finally, it is possible to gain analytic insight into the regime where both the frequency p_0 and μ are kept finite, a situation that can be clearly relevant for experimentally realistic situations. It is easy to see that whenever $|\mu| \leqslant m$ and $p_0 < 2m$, the result is the same as in Eq. (22). However, there is an experimentally more relevant situation when $|\mu| \geqslant m$ but $p_0 < 2m$ still. This is the case of a doped TI at finite frequency. Evaluating $\Pi_5(p_0 \ll 2m, |\mu| > m)$ one obtains the first nontrivial order in p_0:

$$\sigma(p_0,|\mu| > m) = \frac{1}{4}\frac{e^2}{h}\left[\frac{3m}{|\mu|} - \frac{m^3}{|\mu|^3} + \frac{mp_0^2}{6|\mu|^3}\right], \tag{24}$$

which is plotted as a function of the external frequency p_0 for different values of the chemical potential μ in Fig. 3(b). In the limit where $\mu = m$ this coincides with the expansion of Eq. (22) when $p_0 \ll 2m$. In this general case, the quantization of the zero frequency value is also absent for finite values of μ and p_0. Thus our results imply that the Kerr and Faraday rotation[7,8] will turn out not to be quantized in units of the fine-structure constant if the samples are doped and/or if the frequency of the probe is of the order of the surface gap, a common situation in actual experiments.

V. DISCUSSION AND CONCLUSIONS

To summarize, the present findings will inevitably permeate into physically observable quantities whenever optical probes have a frequency comparable to or larger than the surface gap. Given the sizes of the gaps, which are as large as 0.3 eV for the bulk gap and 50 meV for the surface gap,[18,19] it should be possible to observe these effects with infrared probes, which are fully controllable within current state-of-the-art technology.[24] The interplay between both scales can be studied in full lattice models and will be the aim of a subsequent publication.

More elaborate scenarios, such as the proposed repulsive Casimir effect,[9,10] the topological Kerr and Faraday effect,[7,8] or even the optical-modulator device proposed in Ref. 25 should be revisited. These findings can be generalized to other classes of topological materials, such as certain classes of Weyl semimetals that host a Carroll-Field-Jackiw term,[26–29] and also to higher-dimensional analog of TI.

In conclusion we have calculated the electrodynamic response of TI at finite frequencies and finite chemical potential, relating it to the response of a higher-dimensional analog of the anomalous QHE. Beyond reasonable doubt, these findings will permeate and strongly affect physical observables, just like any other finite-frequency response function. We have shown that there is a well-defined action in this case and that it is possible to define a quantity, the total current, which is not sensitive to the particular time-reversal symmetry-breaking profile inside the TI, but it is still dependent on the external frequency characterizing the electromagnetic perturbation. These results pave the way to the understanding topological phenomena at finite frequency, which are bound to be relevant in current experimental setups.

ACKNOWLEDGMENTS

A.G.G. is grateful to A. Cortijo and Shoucheng Zhang for discussions in the early stages of this work. We thank M. A. H. Vozmediano, H. Ochoa, and E. Cappelluti for useful insights. A.G.G. acknowledges support from Spanish Grants No. FIS2008-00124 and No. FIS2011-23713 and Grant No. PIB2010BZ-00512 (Brazil). F.J. acknowledges funding under NSF Grant No. DMR-1005035.

APPENDIX A: CALCULATION OF $\Pi_5(p_0,\mu = 0)$

As described in the main text $\Pi_5(p_0,\mu)$ determines the finite-frequency response of the TI system. In this appendix we provide an alternative derivation starting from the response of a $D = 4 + 1$ system and give details on how to compute it for $\mu = 0$, leaving the $\mu \neq 0$ for Appendix B.

As shown in Ref. 5 the quantized dc magnetoelectric response of TI system can be described as descending from a five-dimensional analog of the quantized integer quantum Hall effect (IQHE).[11] Under this perspective the work of Refs. 12–14 for finite chemical potential can be understood as arising from the corresponding anomalous QHE analog in five dimensions. Similarly, it is possible to reinterpret our results presented in the main text as descending from a five-dimensional finite-frequency QHE at finite chemical potential.

To describe the finite-frequency response of $D = 4 + 1$ at $\mu = 0$ we couple the model to an external electromagnetic field A_μ. After integrating out fermions, we obtain an effective action for the gauge field. This effective action will generate an analog of the QHE described by a Chern-Simons-like term which in momentum space reads

$$S^{\text{eff}}_{4+1} = \int_{\text{BZ}} \frac{d^5q}{(2\pi)^5} \int \frac{d^5p}{(2\pi)^5}\ \Pi_5(p,q)\epsilon^{\mu\nu\rho\sigma\tau} A_\mu p_\nu A_\rho q_\sigma A_\tau, \tag{A1}$$

where $\epsilon^{\mu\nu\rho\sigma}$ is the Levi-Civita totally antisymmetric tensor and A_μ is the electromagnetic gauge field. In real space, the p_μ,q_ν momenta turn into derivatives, and one recovers an action of the form $A\partial A\partial A$, which is a five-dimensional analog of the IQHE action in $D = 2 + 1$ space-time dimensions of the form $A\partial A$. The function $\Pi_5(p,q)$ accounts for the finite-frequency, finite-momentum response of the system. It is generated in perturbation theory from the Feynman diagrams shown in Fig. 1 and can be regarded as arising from the antisymmetric part of the tensor:

$$\Pi_5^{\mu\nu\rho}(p,q) = -ie^2 \int \frac{d^5k}{(2\pi)^5} \text{Tr}[G_{k-p}\Gamma^\mu G_k \Gamma^\nu G_{k-q}\Gamma^\rho + G_{k+p-q}\Gamma^\nu G_k \Gamma^\mu G_{k-q}\Gamma^\rho]. \tag{A2}$$

The electronic Green's function is a function of a five-momentum vector $k = (k_0,\mathbf{k})$, given by $G(k) = [k_0 - H(\mathbf{k})]^{-1}$. For our model with one massive Dirac fermion in $D = 4 + 1$ dimensions[5] the low-energy propagator is of the form

$$G(k) = \frac{k_0 + \Gamma^a k_a}{k_0^2 - \mathbf{k}^2}. \tag{A3}$$

Using the fact that the Γ_a matrices satisfy

$$\text{Tr}\,[\Gamma_a\Gamma_b\Gamma_c\Gamma_d\Gamma_e] = -4\epsilon_{abcde}, \tag{A4}$$

one can isolate in Eq. (A2) the antisymmetric term with five Γ_a matrices to obtain, in terms of the Feynman parameters α,β,γ,[21]

$$\Pi_5^{(a)\mu\nu\rho}(p,q) = -16ie^2 m\epsilon^{\mu\nu\rho\sigma\tau} p_\sigma q_\tau \int \frac{d^5k}{(2\pi)^5} \int_0^1 d\alpha d\beta d\gamma \times \frac{\delta(1-\alpha-\beta-\gamma)}{[k^2 - m^2 + p^2\alpha\beta + q^2\gamma\alpha + (p+q)^2\beta\gamma]^3} \tag{A5}$$

$$= -\frac{e^2m}{8\pi^2}\epsilon^{\mu\nu\rho\sigma\tau} p_\sigma q_\tau \int_0^1 d\alpha d\beta d\gamma \times \frac{\delta(1-\alpha-\beta-\gamma)}{\sqrt{m^2 - p^2\alpha\beta - q^2\gamma\alpha - (p+q)^2\beta\gamma}}$$

$$\equiv \epsilon^{\mu\nu\rho\sigma\tau} p_\sigma q_\tau \Pi_5(q,p). \tag{A6}$$

It is not difficult to check that this definition of $\Pi_5(p,q)$ is analogous to that given in the main text. To compute it, it is possible to numerically evaluate the integrals on the Feynman parameters and find $\Pi_5(q,p)$.

As shown in the main text, it is important to keep in mind that in order to calculate the finite-frequency response to an external time-dependent but spatially uniform electric field, only the external frequency p_0 is kept finite while all the rest are set to zero. The integrals in the Feynman parameters are analytic and give the logarithmic dependence shown in Eq. (22) in the main text.

Consistent with the dc response of a single Dirac fermion,[5] at $p_0 = 0$ the response is quantized to $e^2/2h$, also in agreement with the fact that in the lattice model the integrals span only half of the BZ. The theory recovers the fact that at the boundary of a TI with broken time-reversal symmetry there is a half-integer quantum Hall effect.

APPENDIX B: FINITE CHEMICAL POTENTIAL, $\Pi_5(p_0,\mu)$

In this Appendix we discuss the details of the computation of the response at finite frequency p_0 and chemical potential μ. The integral to be computed in this case is defined in Eq. (A5) with the replacement $k_0 \to k_0 + \mu$:

$$\Pi_5(p,q) = -16ie^2m \int \frac{d^5k}{(2\pi)^5} \int_0^1 d\alpha d\beta d\gamma \times \frac{\delta(1-\alpha-\beta-\gamma)}{[(k_0+\mu)^2 - \mathbf{k}^2 - m^2 + p^2\alpha\beta + q^2\gamma\alpha + (p+q)^2\beta\gamma]^3}. \tag{B1}$$

Following the arguments in the main text the relevant case is where all external momenta are zero except p_0. The integral in k_0 has two third-order poles at $k_0^{\pm}$. The position of the poles in the complex plane is determined by the relative magnitude of m^2, μ, α, p_0, and $\mathbf{k}^2$.

Consider the simple case where $p_0 \to 0$. Following the procedure in Ref. 23, in this case there is a pole which always has a negative imaginary part, no matter what value of $\mathbf{k}$ it has. The other pole, however, depending on $\mathbf{k}$, will change semiplanes, and so for certain values of $\mathbf{k}$ the integral should be split into two. At this point it is possible to identify several cases.

$|\mu| \leqslant m$. In this case both poles are always in different semiplanes, and the integral is proportional to sign(m).

$|\mu| \geqslant m$. In this case it is necessary split the integral on $\mathbf{k}$ into two parts, one from 0 to k^* and the other one from k^* to ∞, where k^* is the value of $\mathbf{k}$ at which the pole changes semiplane, namely, $\sqrt{\mu^2 - m^2}$. The first integral gives zero since both poles are on the same side. The second one is

$$\Pi_5(\mu) = 16e^2 m \int \frac{dk_0}{2\pi} \int_{k^*}^{\infty} k^3 \frac{dk}{(2\pi)^4} 2\pi^2 \times \frac{1}{[(k_0+\mu)^2 - k^2 - m^2]^3}. \quad \text{(B2)}$$

We calculate first the k_0 integral with the residue theorem. It is a third-order pole, so closing the contour from above and restoring $\hbar$, we find

$$\Pi_5(\mu) = \frac{1}{2}\frac{1}{8\pi^2}\left[-\frac{3m}{|\mu|} + \frac{m^3}{|\mu|^3}\right]\frac{e^2}{\hbar}. \quad \text{(B3)}$$

Since we need $\sigma(\mu) \equiv 2\pi\Pi_5(\mu)$, we finally obtain (23):

$$\sigma(\mu) = 2\pi\Pi_5(\mu) = \frac{1}{4}\left[-\frac{3m}{|\mu|} + \frac{m^3}{|\mu|^3}\right]\frac{e^2}{h}, \quad \text{(B4)}$$

which reduces to the familiar $\frac{1}{2}\frac{e^2}{h}$sign(m) contribution of a $2+1$ massive Dirac fermion when $m = \mu$ and has an extra term $\frac{m^3}{|\mu|^3}$ compared to the $D = 2+1$ case.[23] For finite p_0 and $|\mu| \geqslant m$ one can generalize the same arguments and find that for $p_0 \ll 2m$ we have

$$\sigma(p_0 < 2m, \mu) = \frac{1}{4}\left[-\frac{3m}{|\mu|} + \frac{m^3}{|\mu|^3} - \frac{mp_0^2}{6|\mu|^3}\right]\frac{e^2}{h}. \quad \text{(B5)}$$

[1] L. D. Landau and E. M. Lifshitz, *Electrodynamics of Continuous Media* (Pergamon, Oxford, 1984).
[2] W. Eerenstein, N. D. Mathur, and J. F. Scott, Nature (London) **442**, 759 (2006).
[3] X.-L. Qi and S.-C. Zhang, Rev. Mod. Phys. **83**, 1057 (2011).
[4] M. Z. Hasan and C. L. Kane, Rev. Mod. Phys. **82**, 3045 (2010).
[5] X.-L. Qi, T. L. Hughes, and S.-C. Zhang, Phys. Rev. B **78**, 195424 (2008).
[6] A. M. Essin, J. E. Moore, and D. Vanderbilt, Phys. Rev. Lett. **102**, 146805 (2009).
[7] J. Maciejko, X.-L. Qi, H. D. Drew, and S.-C. Zhang, Phys. Rev. Lett. **105**, 166803 (2010).
[8] W.-K. Tse and A. H. MacDonald, Phys. Rev. Lett. **105**, 057401 (2010).
[9] A. G. Grushin and A. Cortijo, Phys. Rev. Lett. **106**, 020403 (2011).
[10] A. G. Grushin, P. Rodriguez-Lopez, and A. Cortijo, Phys. Rev. B **84**, 045119 (2011).
[11] S.-C. Zhang and J. Hu, Science **294**, 823 (2001).
[12] M. Barkeshli and X.-L. Qi, Phys. Rev. Lett. **107**, 206602 (2011).
[13] D. L. Bergman, Phys. Rev. Lett. **107**, 176801 (2011).
[14] D. L. Bergman and G. Refael, arXiv:1201.3042.
[15] C.-X. Liu, X.-L. Qi, H. J. Zhang, X. Dai, Z. Fang, and S.-C. Zhang, Phys. Rev. B **82**, 045122 (2010).
[16] A term of the type $\epsilon(\mathbf{k})\mathrm{I}_{4\times 4}$ can also be included, but it does not affect the topological properties, so we neglect it for simplicity.
[17] Y. Xia, D. Qian, D. Hsieh, L. Wray, A. Pal, H. Lin, A. Bansil, D. Grauer, Y. S. Hor, R. J. Cava, and M. Z. Hasan, Nat. Phys. **5**, 398 (2009).
[18] Y. L. Chen, J.-H. Chu, J. G. Analytis, Z. K. Liu, K. Igarashi, H.-H. Kuo, X. L. Qi, S. K. Mo, R. G. Moore, D. H. Lu, M. Hashimoto, T. Sasagawa, S. C. Zhang, I. R. Fisher, Z. Hussain, and Z. X. Shen, Science **329**, 659 (2010).
[19] L. Andrew Wray, Su-Yang Xu, Yuqi Xia, Yew San Hor, Dong Qian, Alexei V. Fedorov, Hsin Lin, Arun Bansil, Robert J. Cava, and M. Zahid Hasan, Nature Physics **6**, 855 (2010).
[20] D. M. Basko, New J. Phys. **11**, 095011 (2009).
[21] R. Delbourgo and A. B. Waites, Aust. J. Phys. **47**, 465 (1994).
[22] C. L. Kane and E. J. Mele, Phys. Rev. Lett. **95**, 226801 (2005).
[23] A. Cortijo, A. G. Grushin, and M. A. H. Vozmediano, Phys. Rev. B **82**, 195438 (2010).
[24] A. A. Schafgans, K. W. Post, A. A. Taskin, Y. Ando, X.-L. Qi, B. C. Chapler, and D. N. Basov, Phys. Rev. B **85**, 195440 (2012).
[25] R. Li, J. Wang, X.-L. Qi, and S.-C. Zhang, Nature Physics **6**, 284 (2010).
[26] S. M. Carroll, G. B. Field, and R. Jackiw, Phys. Rev. D **41**, 1231 (1990).
[27] L. Balents, Physics **4**, 36 (2011).
[28] A. G. Grushin, Phys. Rev. D **86**, 045001 (2012).
[29] A. A. Zyuzin and A. A. Burkov, arXiv:1206.1868.